J. Phys. Chem. A **1997,** *101,* 6807−6812

Theoretical Studies of $XONO_2-H_2O$ (X = Cl, H) Complexes

Liming Ying and Xinsheng Zhao*

Department of Chemistry, Peking University, Beijing 100871, China

Received: December 16, 1996[⊗]

The equilibrium structures, harmonic vibrational frequencies and binding energies of $ClONO_2-H_2O$ and $HONO_2-H_2O$ complexes have been investigated with ab initio MP2 and density functional B3LYP methods. The B3LYP method performs better than MP2 methods in predicting the vibrational frequencies of both $ClONO_2$ and $HONO_2$. It is found that the $ClONO_2-H_2O$ complex possesses a near C_s symmetry structure. The ZPE corrected binding energies determined at B3LYP/6-311++G(2df,2p) level for $ClONO_2-H_2O$ and $HONO_2-H_2O$ complexes are 2.2 and 7.2 kcal mol^{-1}, respectively. A possible surface-based heterogeneous reaction mechanism of $ClONO_2$ on water−ice surface is proposed.

I. Introduction

Heterogeneous reactions on the surfaces of polar stratospheric cloud (PSC) particles are now believed to play a central role in the ozone depletion which occur at polar latitudes in the springtime.[1−3] The surface-catalyzed reactions convert chlorine-containing reservoir species into photochemically active forms:

$$ClONO_2 + H_2O \rightarrow HOCl + HNO_3 \qquad (1)$$

$$ClONO_2 + HCl \rightarrow Cl_2 + HNO_3 \qquad (2)$$

For instance, reactions 1 and 2 convert chlorine from $ClONO_2$ and HCl to HOCl and Cl_2, which are photolyzed readily and form chlorine-containing radicals capable of catalytically destroying ozone.[1,4]

Experimental studies have indicated that the PSCs which act as catalysts for these reactions consist of either nitric acid trihydrate (type I PSC) or water ice (type II PSC).[5−7] The probabilities of heterogeneous reactions on solid surfaces have been extensively studied. Molina et al.,[8] Tolbert et al.,[9] and Leu[10] reported that reactions 1 and 2 proceed readily on cold water−ice surfaces. Further experiment of Hanson and Ravishankara showed that a pure ice surface can be contaminated with the nitric acid that is produced in the reaction.[11]

Apparently, the knowledge on the gas-phase structures and binding energies of $ClONO_2-H_2O$ and $HONO_2-H_2O$ complexes is essential to the understanding of the mechanism of heterogeneous reactions involving $ClONO_2$. The interaction of $ClONO_2$ with water has been studied by Manna[12] at the Hartree−Fock level with optimization of the geometry parameters directly involved in the interaction (geometry of single molecules are held fixed). It was found that the strongest interaction between $ClONO_2$ and H_2O involves the chlorine atom of $ClONO_2$ and oxygen atom of H_2O. In this paper, we report our theoretical investigations on the molecular structures, vibrational frequencies and binding energies of $ClONO_2-H_2O$ and $HONO_2-H_2O$ complexes. Guided by our calculation, a possible heterogeneous reaction mechanism of $ClONO_2$ on a water−ice surface is proposed.

II. Methods of Calculation

Ab initio and density functional calculations have been performed with the GAUSSIAN 94 programs[13] on a DEC alpha 3000/300 workstation. Three isomers of $ClONO_2-H_2O$ complex are found and geometrically optimized at HF/6-31G(d) level. The structure that possesses the largest binding energy is further optimized at MP2[14] (frozen core) and B3LYP levels with 6-31G(d) and 6-311G(d,p) basis sets. The B3LYP method uses Becke's three-parameter nonlocal exchange functional[15] with the nonlocal correlation functional of Lee, Yang, and Parr.[16] Vibrational frequencies are obtained to determine the nature of stationary points and for the ZPE corrections to the binding energies. Single point energy calculations are performed at the B3LYP level with several larger basis sets. It is estimated that the error in the binding energy at the highest level calculation is 2.0 kcal mol^{-1}.

III. Results and Discussion

A. Chlorine Nitrate and Nitric Acid. It is now generally accepted that $XONO_2$ molecules possess planar structures,[17,19,21] and thus only planar structures of $ClONO_2$ and $HONO_2$ have been investigated. The equilibrium geometries, dipole moments, and rotational constants of $ClONO_2$ and $HONO_2$ obtained at various levels of theory are presented in Tables 1 and 2, respectively. The experimental vibrationally averaged structures, dipole moments and rotational constants are also included for comparison.

For $ClONO_2$, both B3LYP and CCSD(T)[21] methods obtain results in agreement with experiment. The largest discrepancy occurs for the $Cl-O_1$ bond distance, which is 0.03−0.04 Å longer than the experimental value. Lee[21] attributed this difference to the deficiencies of the basis set. There is no substantial effect on the molecular structure when the basis set is increased from 6-31G(d) to 6-311G(d) with both MP2 and B3LYP methods. The B3LYP/6-31G(d) method gives the results of almost the same quality as higher level CCSD(T)/TZ2P method. MP2 method does not work satisfactorily for the O_1-N bond length. The dipole moment of $ClONO_2$ is sensitive to the use of electronic correlation. At the MP2 level using Hartree−Fock density matrix, the calculated values are far from experiment, as can be seen from Table 1. However, if the MP2 density matrix was employed for the dipole moment calculation, Mebel et al.[22] obtained a value of 0.76 D at MP2/6-31G(d) level of theory, in agreement with the experimental value of 0.77 D.[19] On the contrary, Lee[21] suspected the reliability of the experimental dipole moment and suggested a different experimental value based on the agreement between the CCSD(T)/TZ2P level calculation and the experiment on the dipole moment of other molecules including several chlorine contained species. However, we also notice that in this case

---

[⊗] Abstract published in *Advance ACS Abstracts,* July 1, 1997.

S1089-5639(97)00022-4 CCC: $14.00

TABLE 1: Calculated Geometry Parameters, Dipole Moments, and Rotational Constants of ClONO$_2$ (Distance R in angstroms, Bond Angle α in degrees, Dipole Moment in debye, Rotational Constant in MHz)

parameter	MP2/6-31G(d)	MP2/6-311G(d)	B3LYP/6-31G(d)	B3LYP/6-311G(d)	CCSD(T)/TZ2P[b]	expt[a]
R(ClO$_1$)	1.704	1.706	1.710	1.717	1.707	1.673
R(O$_1$N)	1.547	1.541	1.502	1.516	1.511	1.499
R(O$_2$N)	1.203	1.190	1.196	1.186	1.195	1.196
R(O$_3$N)	1.207	1.192	1.199	1.188	1.197	1.196
α(ClO$_1$N)	111.2	112.0	113.2	113.6	111.9	113.0
α(O$_1$NO$_2$)	117.3	117.3	118.0	117.7	117.8	118.6
α(O$_1$NO$_3$)	107.7	107.6	108.4	108.2	108.7	108.8
μ	1.44	1.40	1.01	0.94	1.08	0.77
A_e	11622	11849	11980	12059	11981	12106
B_e	2703	2697	2699	2670	2723	2777
C_e	2193	2197	2203	2186	2218	2258

[a] Vibrationally averaged structure from ref 17, dipole moment from ref 19, and rotational constants from ref 20. [b] From ref 21.

TABLE 2: Calculated Geometry Parameters, Dipole Moments, and Rotational Constants of HONO$_2$ (Distance R in angstroms, Bond Angle α in degrees, Dipole Moment in debye, Rotational Constant in MHz)

parameter	MP2/6-31G(d)	MP2/6-311G(d)	B3LYP/6-31G(d)	B3LYP/6-311G(d)	CCSD(T)/TZ2P[b]	expt[a]
R(HO$_{1)}$	0.983	0.969	0.979	0.971	0.969	0.964
R(O$_1$N)	1.412	1.407	1.410	1.415	1.418	1.406
R(O$_2$N)	1.226	1.213	1.217	1.210	1.216	1.211
R(O$_3$N)	1.216	1.202	1.203	1.194	1.200	1.199
α(ClO$_1$N)	102.2	102.0	102.6	103.0	101.5	102.2
α(O$_1$NO$_2$)	115.7	115.7	115.7	115.6	115.4	115.9
α(O$_1$NO$_3$)	113.6	113.7	113.9	113.9	114.0	113.9
μ	2.74	2.69	2.35	2.31	2.19	2.17
A_e	12643	12909	12878	13031	12909	13011
B_e	11983	12135	12050	12049	11992	12100
C_e	6152	6255	6225	6261	6217	6261

[a] Vibrationally averaged structure, dipole moments, and rotational constants from ref 18. [b] From ref 21.

TABLE 3: Fundamental Vibrational Frequencies (cm^{-1}) and IR Intensities (km/mol) of ClONO$_2$

mode	approx assignment	MP2/6-311G(d)	B3LYP/6-311G(d)	CCSD(T)/TZ2P[b]	expt[a]
A′ ν_1	NO$_2$ asym str	1977(191)	1824(348)	1730(343)	1735 vs
ν_2	NO$_2$ sym str	1332(238)	1351(293)	1298(254)	1292 vs
ν_3	ClO′ str	776(32)	772(6.9)	786(18)	780 ms
ν_4	NO$_2$ scissors	797(178)	824(197)	813(164)	809 s
ν_5	O′N str	532(94)	556(56)	560(56)	560 s
ν_6	O′NO$_2$ ip bend	402(100)	434(19)	434(14)	434 m
ν_7	ClO′N bend	250(1.3)	244(0.3)	256(0.1)	270 vvw
A″ ν_8	O′NO$_2$ op bend	715(9.7)	724(14)	713(9.0)	711 w
ν_9	ClONO torsion	125(0.9)	133(0.6)	122(0.3)	120

[a] From ref 23. [b] From ref 21.

TABLE 4: Fundamental Vibrational Frequencies (cm^{-1}) and IR Intensities (km/mol) of HONO$_2$

mode	approx assignment	MP2/6-311G(d,p)	B3LYP/6-311G(d,p)	CCSD(T)/TZ2P[b]	expt[a]
A′ ν_1	HO′ str	3799(93)	3735(91)	3747(85)	3550 m
ν_2	NO$_2$ asym str	1903(223)	1779(368)	1722(345)	1710 vs
ν_3	HO′N bend	1366(165)	1327(45)	1310(162)	1304 vs
ν_4	NO$_2$ sym str	1350(164)	1359(321)	1349(207)	1326 s
ν_5	NO$_2$ scissors	919(207)	911(185)	895(154)	879 s
ν_6	O′N str	676(9.7)	654(14)	649(9.3)	647 w
ν_7	O′NO$_2$ ip bend	596(10)	588(7.9)	580(9.3)	580 w
A″ ν_8	O′NO$_2$ op bend	770(7.8)	777(12)	761(9.5)	763 s
ν_9	HONO torsion	461(134)	480(134)	469(117)	458 m

[a] From ref 23. [b] From ref 21.

the B3LYP method gives better value of the dipole moment than CCSD(T) method compared to the experiment.

For the geometry parameters of HONO$_2$, all methods give very good results compared to the experiment, except for the MP2/6-31G(d) level, where the H−O$_1$ and O−N bond length are 0.01−0.02 Å too long. The quality of B3LYP/6-311G(d,p) method is essentially the same as CCSD(T)/TZ2P method in this case, but the latter performs better in dipole moment calculation.

Calculated fundamental vibrational frequencies and IR intensities of ClONO$_2$ and HONO$_2$ are tabulated in Tables 3 and 4, along with the observed gas-phase fundamental frequencies.[23] The B3LYP/6-311G(d,p) method well predicts the vibrational frequencies of ClONO$_2$ and HONO$_2$. Mebel et al.[22] have reported the vibrational frequencies of ClONO$_2$ and HONO$_2$ determined at B3LYP/6-31G(d) level recently. Our results at this level are the same as theirs and are omitted here. Among the CCSD(T), B3LYP, and MP2 methods, CCSD(T) gives the best vibrational frequencies of NO$_2$ antisymmetric stretch of both ClONO$_2$ and HONO$_2$ as well as that of H−O stretch of HONO$_2$. The MP2 frequencies are somewhat not satisfying in this case.

B. Structures, Vibrational Frequencies, and Binding Energies of ClONO$_2$−H$_2$O and HONO$_2$−H$_2$O Complexes.

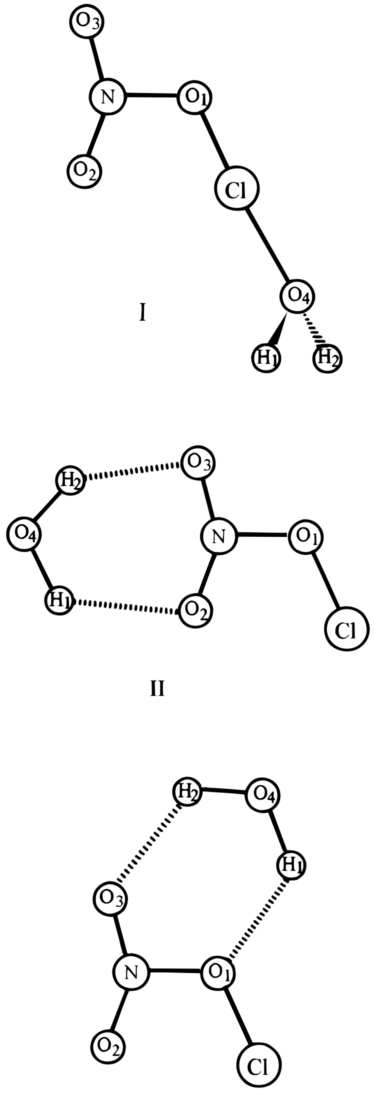

I

II

III

Figure 1. Investigated isomers of the $ClONO_2-H_2O$ complex .

First, three isomers of the $ClONO_2-H_2O$ complex are investigated at the HF/6-31G(d) level, as depicted in Figure 1. The geometries are fully optimized and vibrational frequencies are determined to characterize the nature of stationary points. Although there might exist other isomers, the isomers considered here cover all three types of interaction, i.e., Cl atom of $ClONO_2$ with O atom of water, O_2, O_3 atoms of $ClONO_2$ with H atom of water, and O_1, O_3 (or O_2) atoms of $ClONO_2$ with H atom of water. It is found that isomer **I** whose equilibrium structure has C_s symmetry holds the largest binding energy, while a planar geometry is merely a transition structure. Isomer **II** has a planar structure, and isomer **III** has a nonplanar structure, with ZPE corrected binding energies 3.0 and 1.5 kcal mol^{-1} less than that of isomer **I** at HF/6-31G(d) level, respectively. Thus, the conclusion of Manna[12] that the strongest interaction of $ClONO_2$ with water involves the Cl atom of $ClONO_2$ and O atom of water is confirmed.

The geometry of isomer **I** is further optimized at MP2 and B3LYP levels of theory with 6-31G(d) and 6-311G(d,p) basis sets, and the results are shown in Table 5. It is found that the equilibrium structure of the complex maintains C_s symmetry at the MP2 level but slightly deviates from the C_s symmetry at B3LYP level. The complex has almost linear configuration in O−Cl···O. Upon complexation, the most significant change arises in $Cl-O_1$ and O_1-N bond lengths. Comprehensibly, the $Cl-O_1$ bond lengthens and the O_1-N bond shortens since the Cl atom acts as an electron acceptor. Surprisingly, the B3LYP method predicts 0.02 Å more changes in $Cl-O_1$ bond distance than MP2 method. The intermolecular $Cl\cdots O_4$ distances are 2.52 and 2.65 Å with B3LYP and MP2 methods, respectively, which are almost the same as $BrONO_2-H_2O$ complex at same levels of theory.[24]

TABLE 5: Calculated Geometry Parameters of $ClONO_2-H_2O$ Complex (Distance *R* in angstroms, Bond Angles α and Dihedral Angles δ in degrees)

parameter	MP2/ 6-31G(d)	MP2/ 6-311G(d,p)	B3LYP/ 6-31G(d)	B3LYP/ 6-311G(d,p)
$R(ClO_1)$	1.716	1.717	1.742	1.747
$R(O_1N)$	1.499	1.497	1.458	1.470
$R(O_2N)$	1.209	1.195	1.203	1.194
$R(O_3N)$	1.212	1.197	1.205	1.195
$R(O_4Cl)$	2.648	2.670	2.515	2.526
$R(O_4H_1)$	0.970	0.959	0.971	0.964
$R(O_4H_2)$	0.970	0.959	0.971	0.964
$\alpha(ClO_1N)$	111.9	112.6	113.7	114.2
$\alpha(O_1NO_2)$	118.1	117.9	118.7	118.4
$\alpha(O_1NO_3)$	108.7	108.6	109.6	109.4
$\alpha(O_4ClO_1)$	179.8	180.0	179.8	179.3
$\alpha(H_1O_4Cl)$	106.0	106.4	101.1	105.1
$\alpha(H_2O_4Cl)$	106.0	106.4	101.0	105.0
$\alpha(H_1O_4H_2)$	104.4	103.1	104.5	104.9
$\delta(O_2NO_1Cl)$	0.0	0.0	0.0	−0.1
$\delta(O_3NO_1Cl)$	180.0	180.0	180.0	179.9
$\delta(O_4ClO_1N)$	180.0	180.0	180.1	180.2
$\delta(H_1O_4ClO_1)$	124.7	125.2	124.8	119.1
$\delta(H_2O_4ClO_1)$	−124.7	−125.2	−128.0	−130.6

TABLE 6: Calculated Geometry Parameters of $HONO_2-H_2O$ Complex (Distance *R* in angstroms, Bond Angles α and Dihedral Angles δ in Degrees)

parameter	MP2/ 6-31G(d)	MP2/ 6-311G(d,p)	B3LYP/ 6-31G(d)	B3LYP/ 6-311G(d,p)
$R(H_1O_1)$	1.006	0.991	1.010	1.000
$R(O_1N)$	1.380	1.375	1.376	1.380
$R(O_2N)$	1.236	1.222	1.231	1.223
$R(O_3N)$	1.220	1.207	1.206	1.198
$R(O_4H_1)$	1.717	1.690	1.674	1.675
$R(O_4H_2)$	0.974	0.962	0.975	0.967
$R(O_4H_3)$	0.971	0.959	0.970	0.963
$\alpha(H_1O_1N)$	104.5	104.5	105.2	105.3
$\alpha(O_1NO_2)$	117.2	117.0	117.3	117.0
$\alpha(O_1NO_3)$	114.6	114.7	115.1	115.0
$\alpha(O_4H_1O_1)$	172.2	174.5	170.0	171.5
$\alpha(H_2O_4H_1)$	93.9	98.4	90.5	94.7
$\alpha(H_3O_4H_1)$	115.0	121.8	112.2	118.2
$\alpha(H_2O_4H_3)$	105.2	104.7	105.0	106.0
$\delta(O_2NO_1H_1)$	0.0	0.0	−0.4	0.1
$\delta(O_3NO_1H_1)$	180.0	180.0	179.8	180.2
$\delta(O_4H_1O_1N)$	180.0	180.0	181.2	179.7
$\delta(H_1O_4H_1O_1)$	−2.9	0.4	−3.4	−1.9
$\delta(H_2O_4H_1O_1)$	105.8	113.6	103.1	109.1

The strongest interaction of $HONO_2$ with water must exist in the hydrogen bond of the H atom of $HONO_2$ with the O atom of water, which can be deduced from the charge distributions of the monomers. Thus, only this isomer is investigated and the structures optimized at MP2 and B3LYP levels with 6-31G(d) and 6-311G(d,p) basis sets are shown in Table 6. The equilibrium structure is illustrated in Figure 2. The planar structure of $HONO_2$ in the complex maintains at MP2 level of theory, while it slightly deviates from planar structure at B3LYP level of theory. As expected, the O−H···O configuration is near linear; however, it bends toward the O_2 atom of $HONO_2$ due to the interaction of the H atom of water with the O_2 atom. Only one hydrogen atom of water stretches out of the plane substantially. The hydrogen bond length of the $HONO_2-H_2O$ complex is about 1.68 Å, shorter than that in $HOCl-H_2O$,[25]

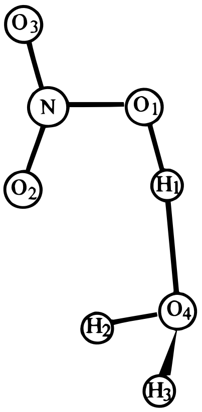

Figure 2. Structure of the $HONO_2-H_2O$ complex.

TABLE 7: Calculated Fundamental Vibrational Frequencies (cm^{-1}) of $ClONO_2-H_2O$ Complex

mode	approx assignment	MP2/ 6-31G(d)	B3LYP/ 6-31G(d)	B3LYP/ 6-311G(d,p)
1	OH_w asym str	3897	3836	3896
2	OH_w sym str	3760	3717	3796
3	NO_2 asym str	1931	1791	1780
4	HOH_w bend	1725	1697	1624
5	NO_2 sym str	1314	1352	1341
6	NO_2 scissors	804	836	839
7	ClO str	775	770	764
8	ONO_2 op bend	711	735	741
9	ON str	565	598	579
10	ONO_2 ip bend	445	445	439
11	ClO_w wag	336	423	420
12	ClON bend	309	405	380
13	$ClOH_w$ rock	261	272	267
14	ClONO torsion	157	176	174
15	ClO_w str	139	175	173
16	dimer torsion	68	77	77
17	dimer rock	66	76	72
18	$ClOH_w$ wag	16	36	25

TABLE 8: Calculated Fundamental Vibrational Frequencies (cm^{-1}) of $HONO_2-H_2O$ Complex

mode	approx assignment	MP2/ 6-31G(d)	MP2/ 6-311G(d,p)	B3LYP/ 6-31G(d)	B3LYP/ 6-311G(d,p)
1	OH_w asym str	3874	3984	3810	3884
2	OH_w sym str	3741	3872	3684	3772
3	HO str	3235	3371	3101	3183
4	NO_2 asym str	1873	1872	1791	1766
5	HOH_w bend	1725	1651	1702	1629
6	HON bend	1537	1536	1518	1498
7	NO_2 sym str	1372	1368	1357	1339
8	ON str	967	974	966	954
9	HO_w wag	907	907	931	917
10	ONO_2 op bend	767	779	780	786
11	NO_2 scissors	687	707	685	691
12	ONO_2 ip bend	650	656	665	654
13	HONO torsion	495	429	547	485
14	HOH_w rock	349	348	372	354
15	HO_w str	243	234	260	245
16	dimer torsion	184	164	211	189
17	dimer rock	148	129	164	139
18	HOH_w wag	78	72	82	79

$HOBr-H_2O$,[24] and H_2O-H_2O.[26] Similarly, the H_1-O_1 bond lengthens and the O_1-N bond shortens upon complexation. Our work indicates that the strength of the interaction between electron donor and electron acceptor plays a central role in $XONO_2-H_2O$ complex conformation.

Harmonic vibrational frequencies have been obtained as shown in Tables 7 and 8. There are only minor changes of the vibrational frequencies of $ClONO_2$. Since the O_1-N bond distance decreases, the O−N stretch frequency increases by 3%. However, things are different for $HONO_2-H_2O$ complex. Significant changes can be seen in several vibrational modes of $HONO_2$. The frequency of the H−O stretch decreases by 550 cm^{-1}, whereas the frequency of the O−N stretch increases by 300 cm^{-1}. Other modes such as NO_2 scissors and ONO_2 in plane bend are affected by O−N stretch. The frequency of the XOH_w wagging mode is also an indication of the interaction strength, which is much higher in $HONO_2-H_2O$ complex than in $ClONO_2-H_2O$ complex.

Tables 9 and 10 show the binding energies of $ClONO_2-H_2O$ and $HONO_2-H_2O$ at various levels of theory, where the binding energies are ZPE corrected. Adding d and f polarization functions reduces binding energy substantially, indicating their importance in the energy calculation. Here, the basis set superposition error (BSSE) may be important, and a complete basis set (CBS)[27] method could be used to accurately calculate the binding energy. However, it would be too time consuming. The binding energies calculated at B3LYP/6-311G(2df,2p)//B3LYP/6-311G(d,p) level are 2.2 and 7.2 kcal mol^{-1} after ZPE correction for $ClONO_2-H_2O$ and $HONO_2-H_2O$ complex, respectively.

C. Proposed Mechanism for Stratospheric Heterogeneous Reactions. The reaction mechanisms of $ClONO_2$ with water and HCl on ice surfaces are not well understood. Wofsy et al.[28] suggested that the reaction of $ClONO_2$ on the surface of PSCs is proton catalyzed. This hypothesis is supported by the ab initio investigation of protonated $ClONO_2$,[29] which indicated that the reaction of proton with $ClONO_2$ proceeds via two steps: proton sticks to $ClONO_2$ to form a $HOCl\cdots NO_2^+$ complex, which dissociates then to HOCl and NO_2^+. Van Doren et al.[30] actually observed the formation of protonated $HONO_2$, known to have the structure $H_2O\cdots NO_2^+$ [31] in the gas-phase reaction of H_3O^+ with $ClONO_2$. It was also found that with one or the other clustered to an NO_3^- core ion, HCl and $ClONO_2$ react efficiently in the gas phase to form $HONO_2$ and Cl_2. In contrast, The NO_3^- ion-assisted neutral reaction of $ClONO_2$ with H_2O to form HOCl and $HONO_2$ was found to be slow.[30] Recently, Mebel et al.[22] has proposed an "attachment−detachment" mechanism for the NO_3^--catalyzed reactions of $ClONO_2$ with HCl, which could also be applied to the proton-catalyzed reaction of $ClONO_2$ with H_2O. Hanson and Ravishankara[32,33] showed that the reaction probability γ for $ClONO_2$ on pure ice to be high on the order of 0.3 and that pure ice surface became contaminated with the nitric acid produced in the reaction. As a result, a decrease in γ of a factor more than 50 occurs. There exists a quite complicated mechanism to explain the decrease of the reaction rate as acidity increases.[34] But, the ion-assisted mechanism does not seem to be satisfactory.

Recently, Hanson[35] investigated the reactivity of $ClONO_2$ on ^{18}O-labeled ice and organic liquids, and evidence for the break of $Cl-ONO_2$ was given. It is also suggested that dissociation or ionization is not prerequisite for heterogeneous reactions of $ClONO_2$ because $ClONO_2$ can efficiently react on the liquid organic surface. On the basis of these results, a six-member-ring transition structure for the reaction was proposed.[35] The enthalpy for reaction 1 is 1 ± 2 kcal mol^{-1},[35] and the energy change of reaction 2 is calculated at MP2/6-31+G(d) level to be −7.8 kcal mol^{-1}.[22] Mebel et al.[22] have found an activation barrier higher than 45 kcal mol^{-1} for the six-member-ring transition structure for reaction 2. Because of the similarity in reaction pattern and heat of reaction, it is expected that if the six-member-ring structure is the transition structure for reaction 1, it would also have sizable barrier, which is too high to account for the large reaction rate constant.

The above mechanisms were established on the basis of pure gas-phase reactions and did not consider the surface and bulk

TABLE 9: Absolute (hartree) and Binding (kcal mol^{-1}) Energies of $ClONO_2-H_2O$ System

theory level	$ClONO_2$	H_2O	$ClONO_2-H_2O$	binding energy
MP2/6-311G(d,p)	−739.286 85	−76.263 97	−815.559 30	3.6
B3LYP/6-311G(d,p)	−740.516 46	−76.447 45	−816.975 87	5.8
B3LYP/6-311++G(2d,p)//MP2/6-311G(d,p)	−740.540 43	−76.459 31	−817.007 07	2.9
B3LYP/6-311++G(2df,2p)//MP2/6-311G(d,p)	−740.553 13	−76.462 40	−817.022 05	2.4
B3LYP/6-311++G(2d,p)//B3LYP/6-311G(d,p)	−740.540 64	−76.459 53	−817.007 38	2.8
B3LYP/6-311++G(2df,2p)//B3LYP/6-311G(d,p)	−740.553 34	−76.462 57	−817.022 00	2.2

TABLE 10: Absolute (hartree) and Binding (kcal mol^{-1}) Energies of $HONO_2-H_2O$ System

theory level	$HONO_2$	H_2O	$HONO_2-H_2O$	binding energy
MP2/6-311G(d,p)	−280.312 82	−76.263 97	−356.597 29	10.6
B3LYP/6-311G(d,p)	−280.967 37	−76.447 45	−357.437 13	11.7
B3LYP/6-311++G(2d,p)//MP2/6-311G(d,p)	−280.987 22	−76.459 31	−357.462 83	7.9
B3LYP/6-311++G(2df,2p)//MP2/6-311G(d,p)	−280.996 53	−76.462 40	−357.474 37	7.4
B3LYP/6-311++G(2d,p)//B3LYP/6-311G(d,p)	−280.987 37	−76.459 53	−357.462 98	7.8
B3LYP/6-311++G(2df,2p)//B3LYP/6-311G(d,p)	−280.996 74	−76.462 57	−357.474 50	7.2

properties. We must bear in mind that the structure of the water−ice surface should play significant roles in the heterogeneous reaction of $ClONO_2$. Up to now, our understanding of the interfacial properties of water is rather primitive. Sum-frequency generation experiments on the air−water interface done by Shen's group[36,37] indicated that about one-fourth of the OH points out of the liquid (free OH bond), and the others are not free. Inspired and guided by our calculation, we propose a possible mechanism concerning the reaction of $ClONO_2$ with water on the ice surface. To reach our proposal, let us first consider the energetics if more water molecules are involved in the reaction, which certainly is the case on the ice surface. If both reactants and products are complexed with water molecules, e.g., if the reaction

$$ClONO_2{\cdot}H_2O + H_2O{\cdot}H_2O \rightarrow HONO_2{\cdot}H_2O + HOCl{\cdot}H_2O \quad (3)$$

is considered, from the ZPE corrected binding energy provided here ($\Delta E[ClONO_2{\cdot}H_2O] = -2.2$ kcal mol^{-1}, $\Delta E[HONO_2{\cdot}H_2O] = -7.2$ kcal mol^{-1}) and other places ($\Delta E[H_2O{\cdot}H_2O] = -3.2$ kcal mol^{-1},[38] $\Delta E[HOCl{\cdot}H_2O] = -5.9$ kcal mol^{-1} [25]) and by assuming that all species on the ice surface were at their most stable complexation, we would estimate that the energy change of reaction 3 were about 7 kcal mol^{-1} more exothermic than that of reaction 1. Next, let us recall a very important well-known fact that the proton transmission through hydrogen bond is very effective in water or ice even at low temperature, because of the low barrier and the proton tunneling. Therefore, if the atoms of both the reactants and the products are at appropriate spatial position, reaction 3 can readily go through a circle bridged by a few water molecules. When putting our calculated geometries and reasonable model of water surface together, it was found that this mechanism could be operative. With this mechanism all aforementioned phenomena can be explained. For example, the reaction need two free surface water molecules, if it is contaminated by $HONO_2$, the reaction will slow. Therefore, as observed, γ for $ClONO_2$ on $HONO_2$-treated ice or NAT (nitric acid trihydrate) is 2−3 orders of magnitude smaller than that on pure ice.[33] In this case, use of the "attachment−detachment" mechanism is difficult to deduce the experimental results, contrarily it may infer that the reaction probability will increase because of the high concentration of $HONO_2$. In addition, our theoretical investigations of $BrONO_2-H_2O$[24] have shown that $BrONO_2$ possesses stronger interaction energy with water. Therefore, the uptake coefficient of $BrONO_2$ on the ice surface may be greater than that of $ClONO_2$. Currently we are investigating the details of the proposed mechanism through ab initio calculation. Preliminary results indicate that the future is promising.

IV. Conclusion

We have investigated the equilibrium structures, harmonic vibrational frequencies and binding energies of $ClONO_2-H_2O$ and $HONO_2-H_2O$ complexes with ab initio MP2 and density functional B3LYP methods. It is shown that B3LYP method performs better than MP2 method in determining the vibrational frequencies of both $ClONO_2$ and $HONO_2$. The most stable form of $ClONO_2-H_2O$ complex possesses C_s symmetry with $ClONO_2$ maintaining a planar structure at the MP2 level of theory but slightly deviates from it at the B3LYP level of theory, in which the oxygen atom of water acts as an electron donor and Cl atom acts as an electron acceptor. The $HONO_2-H_2O$ complex has a structure of almost all atoms lying in a plane except one hydrogen atom of water. The ZPE corrected binding energies determined at B3LYP/6-311++G(2df,2p) level for $ClONO_2-H_2O$ and $HONO_2-H_2O$ complexes are 2.2 and 7.2 kcal mol^{-1}, respectively. A possible surface-based heterogeneous reaction mechanism of $ClONO_2$ on a water−ice surface has been suggested, in which the surface structure of the ice plays a key role. This mechanism is in agreement with the known experimental facts.

Acknowledgment. The authors wish to thank Mr. Sichuan Xu for very stimulating discussions. This work has been supported by NSFC under project No. 29425004.

References and Notes

(1) Solomon, S. *Rev. Geophys.* **1988**, *26*, 131.
(2) Solomon, S.; Garcia, R. R.; Rowland, F. S.; Wuebbles, D. J. *Nature* **1986**, *321*, 755.
(3) Brune, W. H.; Anderson, J. G.; Toohey, D. W.; Fahey, D. W. *Science* **1991**, *252*, 1260.
(4) Anderson, J. G.; Toohey, D. W.; Brune, W. H. *Science* **1991**, *252*, 39.
(5) Toon, O. B.; Hamill, P.; Turco, R. P.; Pinto, J. *Geophys. Res. Lett.* **1986**, *13*, 1284.
(6) Crutzen, P. J.; Arnold, F. *Nature* **1986**, *324*, 651.
(7) Abbatt, J. P. D.; Molina, M. J. *J. Phys. Chem.* **1992**, *96*, 7674.
(8) Molina, M. J.; Tso, T.; Molina, L. T.; Wang, F. C. Y. *Science* **1987**, *238*, 1253.
(9) Tolbert, M. A.; Rossi, M. J.; Malhotra, R.; Golden, D. M. *Science* **1987**, *238*, 1258.
(10) Leu, M. T. *Geophys. Res. Lett.* **1988**, *15*, 17.
(11) Hanson, D. R.; Ravishankara, A. R. *J. Geophys. Res.* **1991**, *96*, 5801.
(12) Manna, G. L. *J. Mol. Struct. (THEOCHEM)* **1994**, *309*, 31.
(13) *Gaussian 94*, Revision B.3; Frisch, M. J.; Trucks, G. W.; Schlegel, H. B.; Gill, P. M. W.; Johnson, B. G.; Robb, M. A.; Cheeseman, J. R.; Keith, T.; Petersson, G. A.; Montgomery, J. A.; Raghavachari, K.; Al-Laham, M. A.; Zakrzewski, V. G.; Ortiz, J. V.; Foresman, J. B.;

Cioslowski, J.; Stefanov, B. B.; Nanayakkara, A.; Challacombe, M.; Peng, C. Y.; Ayala, P. Y.; Chen, W.; Wong, M. W.; Andres, J. L.; Replogle, E. S.; Gomperts, R.; Martin, R. L.; Fox, D. J.; Binkley, J. S.; Defrees, D. J.; Baker, J.; Stewart, J. P.; Head-Gordon, M.; Gonzalez, C.; Pople, J. A.; Gaussian, Inc.: Pittsburgh PA, 1995.

(14) Møller, C.; Plesset, M. S. *Phys. Rev.* **1934**, *46*, 618.

(15) (a) Becke, A. D. *J. Chem. Phys*. **1993**, *98*, 5648. (b) Becke, A. D. *J. Chem. Phys*. **1992**, *96*, 2155. (c) Becke, A. D. *J. Chem. Phys*. **1992**, *97*, 9173.

(16) Lee, C.; Yang, W.; Parr, R. G. *Phys. Rev*. **1988**, *B37*, 785.

(17) Casper, B.; Lambotte, P.; Minkwitz, R.; Oberhammer, H. *J. Phys. Chem*. **1993**, *97*, 9992.

(18) Cox, A. P.; Riveros, J. M. *J. Chem. Phys*. **1965**, *42*, 3106.

(19) Suenram, R. D.; Johnson, D. R. *J. Mol. Spectrosc*. **1977**, *65*, 239.

(20) Suenram, R. D.; Lovas, F. J. *J. Mol. Spectrosc*. **1984**, *105*, 351.

(21) Lee, T. J. *J. Phys. Chem*. **1995**, *99*, 1943.

(22) Mebel, A. M.; Morokuma, K. *J. Phys. Chem*. **1996**, *100*, 2985.

(23) Jacox, M. E. *J. Phys. Chem. Ref. Data* **1994**, *Monograph No. 3*.

(24) Ying, L.; Zhao, X. *J. Phys. Chem. A* **1997**, *101*, 3569.

(25) Dibble, T. S.; Francisco, J. S. *J. Phys. Chem*. **1995**, *99*, 1919.

(26) Xantheas, S. S.; Dunning, T. H., Jr. *J. Chem. Phys*. **1993**, *99*, 8774.

(27) Ochterski, J. W.; Peterson, G. A.; Montgomery, J. A. Jr. *J. Chem. Phys*. **1996**, *104*, 2598.

(28) Wofsy, S. C.; Molina, M. J.; Salawitch, R. J.; Fox, L. E.; McElroy, M. B. *J. Geophys. Res*. **1988**, *93*, 2442.

(29) Lee, T. J.; Rice, J. E. *J. Phys. Chem*. **1993**, *97*, 6637.

(30) Van Doren, J. M.; Viggiano, A. A.; Morris, R. A. *J. Am. Chem. Soc*. **1994**, *116*, 6957.

(31) Lee, T. J.; Rice, J. E. *J. Phys. Chem*. **1992**, *96*, 650.

(32) Hanson, D. R.; Ravishankara, A. R. *J. Geophys. Res*. **1991**, *96*, 5801.

(33) Hanson, D. R.; Ravishankara, A. R. *J. Phys. Chem*. **1992**, *96*, 2682.

(34) See, for example: Molina, M. J.; Molina, L. T.; Kolb, C. E. *Annu. Rev. Phys. Chem.* **1996**, *47*, 327.

(35) Hanson, D. R. *J. Phys. Chem*. **1995**, *99*, 13059.

(36) Du, Q.; Superfine, R.; Freysz, E.; Shen, Y. R. *Phys. Rev. Lett*. **1993**, *70*, 2313.

(37) Du, Q.; Freysz, E.; Shen. Y. R. *Science* **1994**, *264*, 826.

(38) Feyereisen, M. W.; Feller, D.; Dixon, D. A. *J. Phys. Chem.* **1996**, *100*, 2993.